POLITECNICO DI TORINO
Repository ISTITUZIONALE

Selective Removal of Diesel Oil Hydrocarbons in Aerobic Bioremediation

(Article begins on next page)

MDPI

Communication

Selective Removal of Diesel Oil Hydrocarbons in Aerobic Bioremediation

Carla Maria Raffa [1], **Fulvia Chiampo** [1,*], **Andrea Vergnano** [2] **and Alberto Godio** [2]

[1] Department of Applied Science and Technology, Politecnico di Torino, Corso Duca degli Abruzzi 24, 10129 Torino, Italy; carla.raffa@polito.it

[2] Department of Environment, Land and Infrastructure Engineering, Politecnico di Torino, Corso Duca degli Abruzzi 24, 10129 Torino, Italy; andrea.vergnano@polito.it (A.V.); alberto.godio@polito.it (A.G.)

[*] Correspondence: fulvia.chiampo@polito.it; Tel.: +39-011-090-4685

Abstract: In soil bioremediation, the main target is the removal of pollutants to the maximum extent. Careful monitoring of pollution concentration provides information about the process efficacy and removal efficiency. Moreover, a detailed analysis of residual pollution composition provides a detailed picture of single compound removal or presence, especially of interest when pollution is constituted by a mixture of chemical species. This paper shows the first results of a study on the speciation of diesel oil compound removal from soils by aerobic remediation. The experimental study was carried out in a microcosm using indigenous microorganisms and adopting the biostimulation strategy with a mineral salt medium for bacteria. The microcosm contained 200 g of dry soil and 14 g of diesel oil with a carbon to nitrogen ratio (C/N) equal to 180 and water content (u%) equal to 12% by mass. The residual pollution concentration in soil was monitored for 138 days to evaluate both the overall removal efficiency and that for the main groups of hydrocarbons. The results showed that the pollution composition changed during the test because of the different rate of metabolization for the single compounds: the overall removal efficiency was about 65%, and that of different hydrocarbon clusters was between 53% and 88%. The monitoring data also allowed the kinetic study of the degradation process, which was better modeled by a second-order kinetic model than by a first-order one. These findings were confirmed by analyzing other microcosms with different operative conditions (C/N = 120, 180 and u% = 8%, 12%, 15% by mass). The proposed methodology may be useful for the evaluation of compliance to concentration limits imposed by law.

Keywords: aerobic bioremediation; gas-chromatographic analysis; speciation; diesel oil; pollution removal

1. Introduction

Biodegradation by indigenous microorganisms present in the soil is a good technique that permits removing pollutants in contaminated soil. With biostimulation, the optimal dosage of nutrients, such as nitrogen and phosphorus, can be added as a mineral salt medium for bacteria (MSMB) to enhance microbial activity [1].

A detailed knowledge of the pollutant composition is useful to efficiently accomplish bioremediation activity, and for this purpose, a preliminary analytical study is required [2].

The chemical composition of diesel oil is rather complex because of the presence of a huge number of compounds. For this reason, usually, it is advantageous to analyze the main groups of hydrocarbons that constitute the diesel oil, that is to say paraffins, aromatics, naphthenes, and olefins [3], instead of the individual compound concentration.

The common technique for the identification of hydrocarbon species is gas chromatography-mass spectrometry (GC-MS) because it allows us to identify and quantify the chemical compounds [4–6]. However, it is possible to use gas chromatography with a flame ionization detector (GC-FID) and compare the results with a specific standard [7,8]. This allows simplifying the methodological approach without losses of result reliability.

Identifying the removal efficiency for a single hydrocarbon permits improving the degradative process. It is possible to decide to add a specific inoculum to improve the degradation of the hydrocarbons more recalcitrant to removal [9–12] and/or biosurfactants that promote the degradation [13,14]. For example, polycyclic aromatic hydrocarbons can be removed differently by various bacterial strains [15].

We performed a preliminary analysis to identify the hydrocarbon compounds through GC-FID to monitor the degradation of C8–C24 alkanes and aromatic hydrocarbons, including some polycyclic aromatic hydrocarbons (PAHs). The test was done in a microcosm with 200 g of soil, polluted with diesel oil at a concentration of around 70 g kg^{-1} of soil, carbon to nitrogen ratio (C/N) equal to 180, and water content (u%) equal to 12% by mass. The test lasted 138 days, and the findings showed that the removal of the diesel oil components occurred to a different extent. These findings were confirmed by analyzing other microcosms where the operative conditions were C/N = 120 and 180 and u% = 8%, 12%, 15% by mass.

2. Materials and Methods

2.1. Microcosm Properties

The bioremediation process was studied using uncontaminated sandy soil, taken from the landfarming site. The soil had granulometry between 0.15–2 mm; porosity = 40–42% by volume; grain density = 2700 kg m^{-3}; water content in dry condition = 1.3–1.5% by volume [16]. The microcosms had a mass of 200 g of dry soil, contaminated with 14 g of commercial diesel oil, and hydrated with a mineral salt medium for bacteria (MSMB) to obtain the following:

- C/N = 180 and u% = 12% by mass;
- C/N = 120 and u% = 8% by mass.

The MSMB was a water solution containing the following salts: $(NH_4)_2HPO_4$, NH_4NO_3, KH_2PO_4, $K_2HPO_4 \cdot H_2O$, $MgSO_4 \cdot 7H_2O$, $CuSO_4 \cdot 4H_2O$, $MnSO_4 \cdot H_2O$, $FeSO_4 \cdot 7H_2O$, $CaCl_2 \cdot 2H_2O$. The different C/N ratios were achieved by changing the ammonium salt concentration.

The details of the bioremediation test are contained in a previous paper [17].

The tested microcosms were monitored for 138 days, and the diesel oil concentration was measured after 7, 15, 70, 112, 131, and 138 days from the beginning of the test.

2.2. Analysis of Diesel Oil

The diesel oil concentration in the microcosm was estimated using the solvent extraction standardized by the Environmental Protection Agency (EPA) method 3546 (moisture 15–30% by mass) [18], based on microwave heating. In this method, 2 g of the microcosm soil was mixed with 30 mL of solvent (acetone and *n*-hexane with ratio 1:1 by volume) and 2 g of anhydrous sodium sulphate, added to dry the soil. The sample was heated at 110 °C and power 1100 W for 15 min through microwaves, was kept at a constant temperature of 110 °C and power 1100 W for 10 min, and then it was cooled for 20 min. After the extraction, the sample was filtered through a 0.45 μm filter. This procedure was replicated, thus obtaining two extracts.

The diesel oil concentration was quantified using gas chromatography (GC-FID), with the EPA method 8015 [19]. The gas chromatograph was equipped with a flame ionization detector and a DB-5 fused silica capillary column, operated with helium as the carrier and with injector and detector maintained at 220 °C and 250 °C, respectively. The following temperature program was used: initial temperature of 50 °C, ramp to 320 °C at 8 °C min^{-1}, and a constant temperature of 320 °C for 40 min.

The chromatogram was analyzed evaluating the peaks between 6 and 33 min, since this time range contains the characteristic peaks of diesel oil.

The residual diesel oil concentration was calculated using a calibration line achieved with the commercial diesel oil used in the test.

The compounds that characterize the diesel oil were identified by standard kits, namely

- C7—C30 saturated alkanes, 1000 μg/mL each component in hexane;

- PAHs - Polyclic Aromatic Hydrocarbons (acenaphthylene, anthracene, benzo(α)anthracene, fluorene, phenanthrene, pyrene), 500 µg/mL each component in acetone.

Comparing the retention times of the analyzed peaks to the standard ones, the *n*-alkanes from C8 to C24 and six PAHs (namely, acenaphthylene, fluorene, phenanthrene, anthracene, pyrene, and benzo(α)anthracene) were determined.

Two gas chromatographic analyses were performed for each extract.

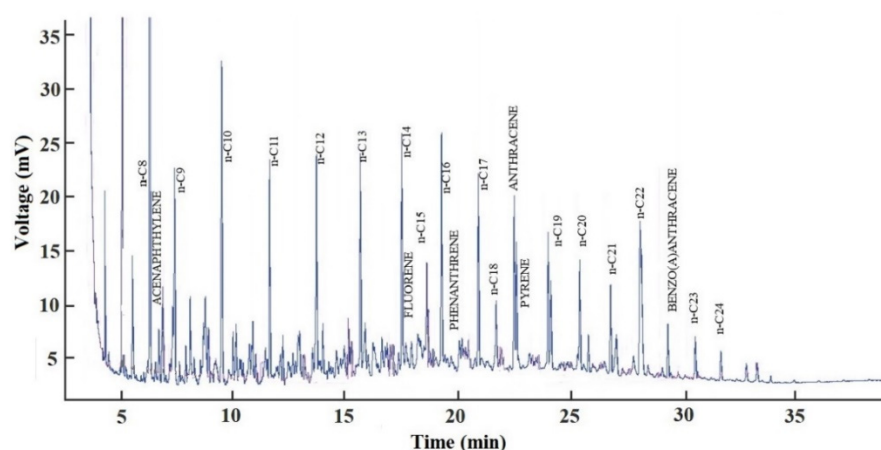Figure 1 reports the chromatogram of the tested commercial diesel oil.

Figure 1. Chromatogram of the commercial diesel oil used in the study.

2.3. Removal Efficiency

The overall pollutant removal efficiency, η, was calculated as

$$\eta = (C_0 - C_1)/C_0 \cdot 100 \tag{1}$$

where C_0 and C_1 are, respectively, the initial diesel oil concentration and the one at the end of the test.

In the same way, the percentage of degraded hydrocarbon species, η_i, was determined as

$$\eta_i = (C_{i,0} - C_{i,1})/C_{i,0} \cdot 100 \tag{2}$$

where $C_{i,0}$ and $C_{i,1}$ are, respectively, the initial hydrocarbon concentration and the one at the end of the test, and i is the specific compound.

The diesel oil removal is carried out mainly by the indigenous microorganisms. To verify this, in a past study [20] done with the same soil and diesel oil, a control abiotic microcosm was also tested. The findings demonstrated that a limited amount of pollutant was removed in this microcosm during the first period of biodegradation. The overall removal efficiency reflects this quantity.

2.4. Kinetic Modeling

Knowing the hydrocarbon concentration, the kinetics of the pollution degradation can be evaluated with the first- and the second-order models. These models derive from the following law:

$$dC/dt = -kC^n \tag{3}$$

where C is the residual diesel oil, k is the reaction rate, and n is the reaction order.

These are typical kinetic models for hydrocarbon degradation [21–24], since they fit well the experimental data.

In both cases, the kinetic constant (k) can be derived by modeling the experimental data achieved by test monitoring.

The half-life time ($t_{1/2}$) is the time required to reduce the concentration of a compound to half of the initial one. For the first-order model (n = 1), it is

$$t_{1/2} = (\ln 2)/k = 0.693/k \qquad (4)$$

For the second-order model (n = 2), the half-life time is

$$t_{1/2} = 1/(kC_0) \qquad (5)$$

The modeling was detailed in a previous study [17].

3. Results

3.1. Identification of Diesel Oil Hydrocarbons

Diesel oil is a distillate containing different compounds including *n*-alkanes (from C8 to C24), branched alkanes, cycloalkanes, and aromatic hydrocarbons. Each chromatogram was compared with the chromatograms of standards, which were obtained with GC-FID analysis under the same operative conditions.

Considering the retention time, the hydrocarbon species were identified in the order shown in Table 1.

Table 1. Identified hydrocarbons and their retention time.

Compound	Retention Time (min)
n-C8	6.3
Acenaphthylene	6.5
n-C9	7.6
n-C10	8.3
n-C11	10.3
n-C12	12.3
n-C13	14.3
n-C14	16.0
Fluorene	17.1
n-C15	17.8
n-C16	19.4
Phenanthrene	20.2
n-C17	20.9
n-C18	21.0
Anthracene	22.4
Pyrene	22.5
n-C19	23.8
n-C20	25.1
n-C21	26.4
n-C22	27.6
Benzo(α)anthracene	28.8
n-C23	29.9
n-C24	31.0

Diesel oil is composed of 65–70% saturated hydrocarbons and 30–35% aromatic ones. By the standards, it was possible to identify the *n*-alkanes and the PAHs, which represent 35% and 10% of the total compounds, respectively.

Table 2 reports the average distribution of the diesel oil components from literature data [25,26] and the value taken as reference for this study.

Table 2. Composition of commercial diesel oil: average values and reference for this study.

Compound	Composition (% by Mass)	
	Range	Adopted Value
Paraffins	9.0–49.0	16.4
Monocycloparaffins	9.5–34.0	14.6
Dicycloparaffins	10.0–32.5	13.8
Tricycloparaffins	0.7–41.5	9.5
Tetracycloparaffins	0.0–3.0	2.9
Alkylbenzenes	2.8–29.0	3.5
Benzocycloparaffins	2.5–18.0	2.6
Benzodicycloparaffins	0.0–14.0	3.6
Naphtalenes	0.0–7.5	6.1
$C_nH_{(2n-14)}$	0.0–5.5	3.6
$C_nH_{(2n-16)}$	0.0–8.5	4.7
Triaromatics	0.0–8.5	2.5
Aromatic sulfur compounds	0.0–6.0	2.3

Referring to Table 2 and integrating our GC-FID analysis, the chemical composition of hydrocarbons was determined considering the number of carbon atoms. The composition of hydrocarbons from C9 to C24 was calculated summing the area of peaks contained between two linear paraffines. For example, for C9 compounds, the integration was done between the *n*-C8 peak and the *n*-C9 one, and so on for the other compounds.

The diesel oil composition by hydrocarbons based on carbon number is shown in Table 3, at the beginning (t = 0 days) and the end (t = 138 days) of the bioremediation process. The data are related to the studied microcosm, with C/N = 180 and u% = 12% by mass.

Table 3. Chemical composition (% by mass and $g\ kg^{-1}$ of soil) of diesel oil by number of carbon atoms, at the beginning (t = 0 days) and the end (t = 138 days) of the experimental run.

Compound	Chemical Composition (% by Mass)		Composition ($g\ kg^{-1}$ of Soil)	
	At t = 0 Days	At t = 138 Days	At t = 0 Days	At t = 138 Days
C8	1.6	2.2	1.0	0.5
C9	3.3	1.0	2.0	0.2
C10	8.0	1.6	4.9	0.3
C11	10.6	4.6	6.5	0.9
C12	9.8	12.2	6.0	2.5
C13	11.2	8.9	6.9	1.8
C14	14.5	17.5	8.9	3.6
C15	7.8	11.5	4.8	2.4
C16	9.2	7.7	5.6	1.6
C17	4.6	6.9	2.8	1.4
C18	3.4	5.3	2.1	1.1
C19	4.9	5.1	3.0	1.0
C20	6.6	6.0	4.1	1.2
C21	1.9	1.5	1.2	0.3
C22	1.3	2.1	0.8	0.4
C23	1.2	4.9	0.7	1.0
C24	0.3	1.0	0.2	0.2

Looking at Table 3, the following points are considered. In commercial diesel oil, the compounds with C14 have the highest concentration, which is kept also at the end of the biodegradation test (t = 138 days). The data show that diesel oil is mainly composed of compounds C10–C16. Considering the composition at the test end (t = 138 days), the compounds with C12–C20 have the highest concentration, and this means that the biodegradative process affects the compounds to a different extent.

Considering the literature data [25,26] and the GC-FID analysis, the composition of the tested diesel oil versus the number of carbon atoms can be given by mass and by concentration in soil, as reported in Table 3. Moreover, the analytical data were grouped by *n*-alkanes, branched alkanes, cycloalkanes, and aromatic hydrocarbons, and their distribution versus the number of carbon atoms is shown in Figure 2.
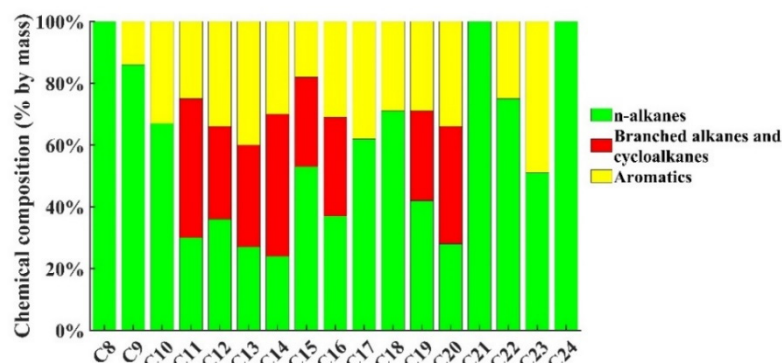

Figure 2. Distribution of *n*-alkanes, branched alkanes, cycloalkanes, and aromatic hydrocarbons versus the number of carbon atoms (t = 0 days).

Figure 2 shows that branched alkanes and cycloalkanes are mainly hydrocarbons with C11–C16 and C19–C20. The aromatic compounds are present in almost all the hydrocarbon fractions, and the highest concentration (49% by mass) occurs in the C23 fraction. The identified PAHs with the standards have 12, 13, 14, 16, and 18 carbon atoms and represent about 7–30% of the total quantity of aromatics with the same number of carbon atoms (this is evidenced by Figure 2, where the aromatics are presented altogether).

Table 3 also shows the chemical composition of the residual diesel oil at the end of the biodegradation process, namely after 138 days from the beginning of the test.

At t = 0 days, the distribution of-alkanes, branched alkanes, cycloalkanes, and aromatic hydrocarbons by the number of carbon atoms is shown in Figure 3.
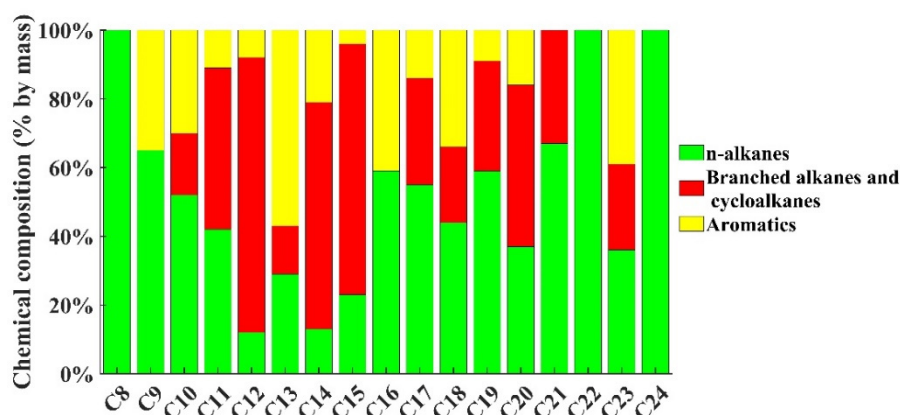

Figure 3. Distribution of *n*-alkanes, branched alkanes, cycloalkanes, and aromatic hydrocarbons versus the number of carbon atoms (t = 138 days).

In the test, the differences between two diesel oil compositions depends on the degradation rate of each compound and the formation of co-metabolites during the process. For example, the final composition of C10 contains 18% of branched alkanes and cycloalkanes, which were not present in the initial composition. The same happens for C17, C18, C21, and C23.

3.2. Removal Efficiency

The identification of peaks allowed evaluating the degradation of a single hydrocarbon, according to Equation (2). For more practical usability, we preferred to show the results by grouping the alkanes into four clusters (C8-C11; C12–C15; C16–C19; C20–C24), while for the aromatic hydrocarbons the overall degradation efficiency was reported.

The removal efficiency for four hydrocarbon clusters and aromatics, η_H, can be calculated with the summation:

$$\eta_H = \sum_{1}^{n} \eta_i \tag{6}$$

where n is the last hydrocarbon compound of each cluster.

Figure 4 reports the results for the tested microcosm.
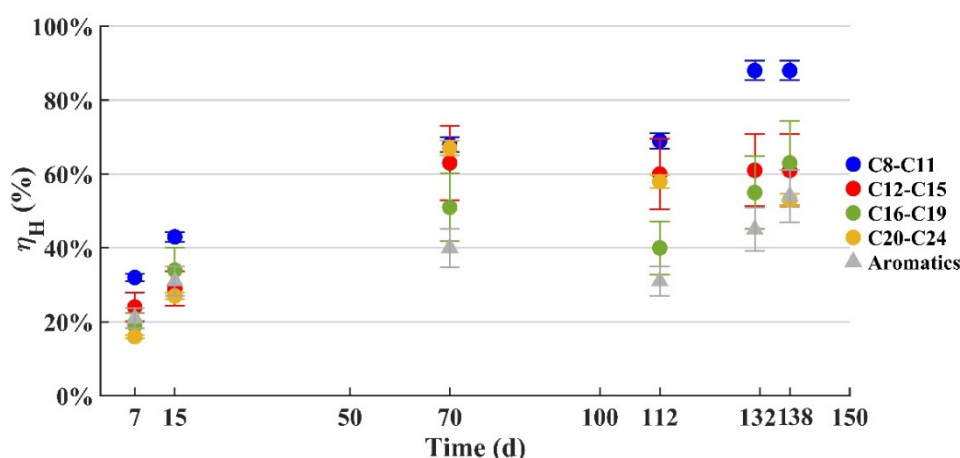

Figure 4. Removal efficiency of hydrocarbon clusters. Relative standard deviation range: 1.91–12.91%.

In general, the trend of the removal efficiency was similar for all hydrocarbon clusters, the percentage of removal increased much in the first 70 days; then, between the 71st and the 138th day, η_H became almost constant. From Figure 4, it is evident that the hydrocarbons with short chains (alkanes C8–C11) were the most degraded, while as the number of carbon atoms increased, the removal efficiency decreased.

The C8–C11 cluster was reduced by 30% after 7 days from the beginning of the test and over 80% after 138 days. The trend of the removal efficiency for this cluster was always higher than for the others.

The removal efficiency of the C12–C15 cluster was equal to 63%, and this percentage remained unchanged from the 70th day to the end.

The C16–C19 cluster showed an evident minimum at t = 112 days: this means that at this time, its concentration was higher than at t < 112 days. As a hypothesis, the reason could be the generation of C16–C19 compounds deriving from the degradation of compounds with a higher carbon number.

From the starting time to the 112th day, the removal kinetics for the C20–C24 compounds were very similar to those of the C12–C15 compounds.

The removal trend of aromatic hydrocarbons was slower than for the other compounds, due to the molecular complexity and their difficulty to be degraded.

3.3. Kinetic Modeling

The removal kinetics of the previously considered clusters were interpreted with first- and second-order models.

In both models, the kinetic constant (k) and the half-life time ($t_{1/2}$) were calculated, considering the hydrocarbon concentrations at t = 0, 7, 15, and 70 days.

Regarding the first-order model, the concentration of hydrocarbon compounds (C_H) versus time is shown in Figure 5, and the parameters k and $t_{1/2}$, which describe the kinetics, are reported in Table 4.
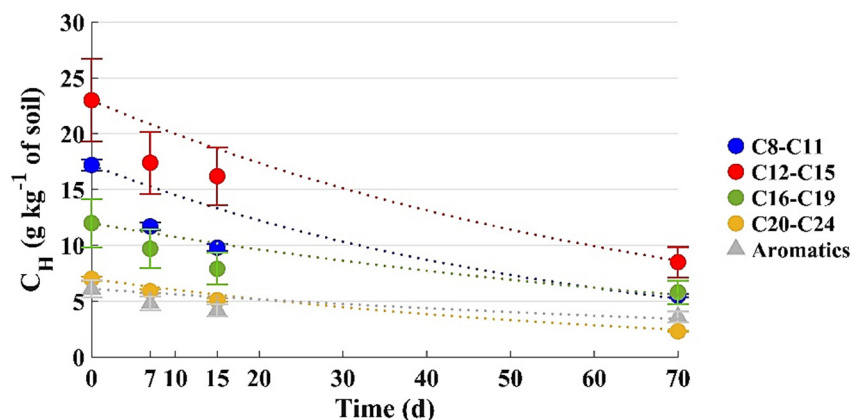

Figure 5. First-order model. Relative standard deviation range: 2.79—14.95%.

Table 4. First-order reaction rate constants and half-life times.

Compounds	k (d^{-1})	R^2	t$_{1/2}$ (d)
C8–C11	0.017	0.81	42
C12–C15	0.014	0.94	49
C16–C19	0.011	0.67	60
C20–C24	0.015	0.99	45
Aromatics	0.0083	0.33	84

Looking at Figure 5 and R^2 in Table 4, it possible to see that for the clusters C8–C11, C12–C15, and C20–C24, this model fits well the experimental data, while in the other cases the results are not well interpreted ($R^2 < 0.8$). The half-life time is in line with the removal trend (Figure 4). Almost all the compounds, except aromatics, were reduced by more than 50% after 70 days (their calculated half-life time is between 42 and 60 days).

The concentration of the hydrocarbon clusters, described with the second-order model, is reported in Figure 6, and the kinetic parameters are shown in Table 5.
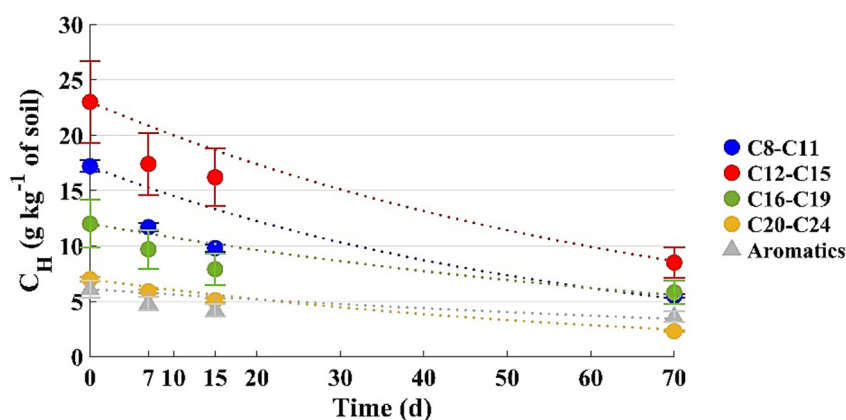

Figure 6. Second-order model. Relative standard deviation range: 2.79–14.95%.

Table 5. Second-order reaction rate constants and half-life times.

Compounds	k (kg g^{-1} d^{-1})	R^2	$t_{1/2}$ (d)
C8–C11	0.0018	0.94	32
C12–C15	0.0011	0.97	40
C16–C19	0.0013	0.84	64
C20–C24	0.0041	0.99	35
Aromatics	0.0018	0.47	92

The second-order model interprets the data better than the first-order one: R^2 was lower than 0.8 only for the aromatics. The half-life time was lower than with the first-order model, in agreement with the trend of removal efficiency.

3.4. Application of Method for Other Microcosms

To support the findings, the method to quantify the hydrocarbon fractions was also applied to several microcosms with the same diesel oil concentration but different operative conditions, namely u% = 8%, 12%, and 15% by mass and C/N = 120 and 180, studied in previous tests with other aims [17].

As an example, Table 6 shows the removal efficiency of diesel oil in the microcosms with C/N = 120 and 180 with different water content.

Table 6. Diesel oil removal efficiency η by microcosms with C/N = 120 and 180 at t = 138 days.

u% (by Mass)	C/N = 120			C/N = 180		
	8%	12%	15%	8%	12%	15%
η %	72%	63%	68%	52%	65%	59%

The highest η value (72%) was obtained in the microcosm with C/N = 120 and u% = 8% by mass; in the other cases, the diesel oil removal was lower than 70%.

Table 7 reports the removal efficiency of hydrocarbon species, η_H, in the microcosms with C/N = 120 and 180 for the aforesaid clusters (C8–C11, C12–C15, C16–C19, C20–C24, aromatics).

Table 7. Removal efficiency, η_H, for the hydrocarbon clusters and aromatics in the microcosms with C/N = 120 and 180 after 138 days.

u% (by Mass)	C/N = 120			C/N = 180		
	8%	12%	15%	8%	12%	15%
C8–C11	76%	79%	78%	72%	88%	74%
C12–C15	69%	68%	65%	51%	61%	60%
C16–C19	69%	52%	60%	35%	63%	51%
C20–C24	68%	44%	68%	57%	53%	61%
Aromatics	84%	47%	45%	41%	54%	29%

The C8–C11 hydrocarbon cluster showed the highest removal efficiency, between 72% and 88%.

4. Discussion

We paid attention to the identification of hydrocarbons and determined the removal efficiency of diesel oil (η) and single hydrocarbon compounds (η_H).

The results are significant: comparing our data with those obtained by Chen et al. [6], who used GC-MS, the percentage of removal of the same hydrocarbon clusters was very similar, even if their test duration was longer (t = 210 days). Masy et al. [27] confirmed that for the identification of these compounds, the GC-FID analysis generates results in line with those obtained with GC-MS. They achieved the same hydrocarbon removal efficiency as in our study, using similar test durations.

In our tested microcosms, the removal efficiency was higher for the alkanes with a medium-length chain than for those with a long-length chain. From our findings (Table 7), the degradation of the C8–C11 cluster was in the range between 72% and 88%, namely the highest. For the other clusters, the efficiency was always lower than 70%.

In terms of overall removal efficiency, the microcosm with C/N = 120 and u% = 8% by mass gave the highest value, equal to 72%. At the same time, this microcosm also gave the highest values of degradation (η_H) for each cluster.

It was noted that the removal trend for aromatic hydrocarbons (Figure 4) was slower than for the other compounds. Considering the retention times shown in Table 1 and the composition of diesel oil based on carbon atoms (Table 3), it is possible to observe that, except for acenaphthylene, the PAHs were removed after the *n*-C16 compound. Thus, the removal trend for the aromatic hydrocarbons below the heaviest hydrocarbon cluster (C20–C24) reflects the molecular complexity and their difficulty to be degraded.

The low molecular mass compounds are preferentially degraded; thereby, the concentrations of fractions with C10–C12 and C12–C16 are removed [28]. This is due to the lower hydrophobicity of the short and medium-chain alkanes; thus, they are more easily degraded, as other authors confirmed [9]. The percentage of removed hydrocarbons was 63% on average for alkanes and 50% for aromatics in 138 days, which is in line with the values obtained in other studies [5,29].

Knowledge of the residual diesel oil composition permits evaluating whether the compound concentrations are lower than those stated in the current legislation for remediated soils. For example, Table 8 presents the maximum concentrations of some hydrocarbons allowed by the current Italian legislation [30], showing that the maximum concentration depends on the specific use of the site. Table 8 also reports the concentrations of the pollutants present in the studied soil (microcosm with C/N = 120 and u% = 8% by mass) at the beginning and the end of the process.

Table 8. Maximum concentration of hydrocarbons according to site use compared with study results.

	Maximum Allowed Concentration		Concentration in the Tested Soil		
	Site for Public Use (g kg^{-1} of Soil)	Site for Industrial and Commercial Use (g kg^{-1} of Soil)	At t = 0 Days (g kg^{-1} of Soil)	At t = 138 Days (g kg^{-1} of Soil)	η (%)
Light hydrocarbons (C ≤ 12)	0.010	0.25	25	4.9	80.4%
Heavy hydrocarbons (C > 12)	0.050	0.75	28	8.6	69.3%
Pyrene	0.0050	0.050	0.86	0.056	93.5%
Benzo(α)anthracene	0.00050	0.010	0.53	0.17	67.9%

Looking at the data in Table 8, it is evident that the biological process was not efficient enough to make the site suitable for reuse, despite the high values of removal efficiency; therefore, additional treatment for soil clean-up is compulsory.

5. Conclusions

This study aimed to identify the composition of diesel oil and the estimation of the degradation of hydrocarbon fractions during a bioremediation process. After 138 days, the removal of the hydrocarbons of the tested microcosm (C/N = 180 and u% = 12% by mass) was in the range 53–88% for alkanes, and 54% for aromatics. As expected, the percentage of removal depends on the complexity of the molecules. In particular, the removal efficiency decreases as the complexity of the hydrocarbon chain increases. This trend was confirmed in other tested microcosms.

The kinetic study showed that the degradation process of the hydrocarbon compounds was better represented by a second-order kinetic model than by a first-order one.

The determination of the diesel oil composition and the quantification of hydrocarbon clusters can be useful to verify whether a remediation process is efficient enough for a polluted soil, as per current legislation.

References

1. Maddela, N.R.; Scalvenzi, L.; Pérez, M.; Montero, C.; Gooty, J.M. Efficiency of Indigenous Filamentous Fungi for Biodegradation of Petroleum Hydrocarbons in Medium and Soil: Laboratory Study from Ecuador. *Bull. Environ. Contam. Toxicol.* **2015**, *95*, 385–394. [CrossRef]
2. Arjoon, K.; Speight, J.G. Chemical and Physical Analysis of a Petroleum Hydrocarbon Contamination on Soil Sample to Determine Its Natural Degradation Feasibility. *Inventions* **2020**, *5*, 43–doi:10. [CrossRef]
3. Speight, J.G. *Handbook of Petroleum Product Analysis*; John Wiley & Sons, Inc.: Hoboken, NJ, USA, 2002; pp. 184–188, ISBN 0-471-20346-7.
4. Alisi, C.; Musella, R.; Tasso, F.; Ubaldi, C.; Manzo, S.; Cremisini, C.; Sprocati, A.R. Bioremediation of diesel oil in a co-contaminated soil by bioaugmentation with a microbial formula tailored with native strains selected for heavy metals resistance. *Sci. Total Environ.* **2009**, *407*, 3024–3032. [CrossRef] [PubMed]
5. Wang, Y.; Li, F.; Rong, X.; Song, H.; Chen, J. Remediation of Petroleum-contaminated Soil Using Bulrush Straw Powder, Biochar and Nutrients. *Bull. Environ. Contam. Toxicol.* **2017**, *98*, 690–697. [CrossRef] [PubMed]
6. Chen, F.; Li, X.; Zhu, Q.; Ma, J.; Hou, H.; Zhang, S. Bioremediation of petroleum-contaminated soil enhanced by aged refuse. *Chemosphere* **2019**, *222*, 98–105. [CrossRef] [PubMed]
7. Papazova, D.; Pavlova, A. Development of a Simple Gas Chromatographic Method for Differentiation of Spilled Oils. *J. Chromatogr. Sci.* **1999**, *37*, 1–4. [CrossRef]
8. Ivanova, L.V.; Koshelev, V.N.; Burov, E.A. Influence of the Hydrocarbon Composition of Diesel Fuels on Their Performance Characteristics. *Pet. Chem.* **2014**, *54*, 466–472. [CrossRef]
9. Ghazali, F.M.; Rahman, R.N.Z.A.; Salleh, A.B.; Basri, M. Biodegradation of hydrocarbons in soil by microbial consortium. *Int. Biodeterior. Biodegrad.* **2004**, *54*, 61–67. [CrossRef]
10. Mariano, A.P.; Kataoka, A.P.A.G.; de Angelis, D.F.; Bonotto, D.M. Laboratory study on the bioremediation of diesel oil contaminated soil from a petrol station. *Braz. J. Microbiol.* **2007**, *38*, 346–353. [CrossRef]
11. Brzeszcz, J.; Kapusta, P.; Steliga, T.; Turkiewicz, A. Hydrocarbon Removal by Two Differently Developed Microbial Inoculants and Comparing Their Actions with Biostimulation Treatments. *Molecules* **2020**, *25*, 661. [CrossRef]
12. Gutiérrez, E.J.; Abrahama, M.R.; Baltazar, J.C.; Vázquez, G.; Delgadillo, E.; Tirado, D. *Pseudomonas fluorescens*: A Bioaugmentation Strategy for Oil-Contaminated and Nutrient-Poor Soil. *Int. J. Environ. Res. Public Health* **2020**, *17*, 6959. [CrossRef]
13. Patowary, R.; Patowary, K.; Kalita, M.C.; Deka, S. Application of biosurfactant for enhancement of bioremediation process of crude oil contaminated soil. *Int. Biodeterior. Biodegrad.* **2018**, *129*, 50–60. [CrossRef]
14. Joe, M.M.; Gomathi, R.; Benson, A.; Shalini, D.; Rengasamy, P.; Henry, A.J.; Truu, J.; Truu, M.; Sa, T. Simultaneous Application of Biosurfactant and Bioaugmentation with Rhamnolipid-Producing *Shewanella* for Enhanced Bioremediation of Oil-Polluted Soil. *Appl. Sci.* **2019**, *9*, 3773. [CrossRef]
15. Seo, J.-S.; Keum, Y.-S.; Li, Q.X. Bacterial Degradation of Aromatic Compounds. *Int. J. Env. Res. Public Health* **2009**, *6*, 278–309. [CrossRef] [PubMed]
16. Vergnano, A.; Godio, A.; Raffa, C.M.; Chiampo, F.; Bosco, F.; Ruffino, B. Time domain reflectometry (TDR) monitoring at lab scale of aerobic degradation of diesel oil in a contaminated soil. *Appl. Sci.* **2019**, *9*, 5487. [CrossRef]
17. Raffa, C.M.; Chiampo, F.; Godio, A.; Vergnano, A.; Bosco, F.; Ruffino, B. Kinetics and optimization by response surface methodology of aerobic bioremediation. Geoelectrical parameter monitoring. *Appl. Sci.* **2020**, *10*, 405. [CrossRef]
18. Environmental Protection Agency. *Method 3546 "Microwave Extraction"*; Environmental Protection Agency: Georgetown, Guyana, 2007.

19. Environmental Protection Agency. *Method 8015 "Nonhalogenated Organics Using GC/FID"*; Environmental Protection Agency: Georgetown, Guyana, 2003.

20. Bosco, F.; Casale, A.; Chiampo, F.; Godio, A. Removal of diesel oil in soil microcosms and implication for geophysical monitoring. *Water* **2019**, *11*, 1661. [CrossRef]

21. Agarry, S.E.; Aremu, M.O.; Aworanti, O.A. Kinetic Modelling and Half-Life Study on Enhanced Soil Bioremediation of Bonny Light Crude Oil Amended with Crop and Animal-Derived Organic Wastes. *Pet. Environ. Biotechnol.* **2013**, *4*, 1–11. [CrossRef]

22. Agarry, S.; Latinwo, G.K. Biodegradation of diesel oil in soil and its enhancement by application of bioventing and amendment with brewery waste effluents as biostimulation-bioaugmentation agents. *J. Ecol. Eng.* **2015**, *16*, 82–91. [CrossRef]

23. Ortega, M.F.; García-Martínez, M.-J.; Bolonio, D.; Canoira, L.; Llamas, J.F. Weighted linear models for simulation and prediction of biodegradation in diesel polluted soils. *Sci. Total Environ.* **2019**, *686*, 580–589. [CrossRef] [PubMed]

24. Yaman, C. Performance and Kinetics of Bioaugmentation, Biostimulation, and Natural Attenuation Processes for Bioremediation of Crude Oil-Contaminated Soils. *Processes* **2020**, *8*, 883. [CrossRef]

25. Baldrich, C.A. Diesel characterization by high resolution mass spectrometry-gas chromatography. *CT&F—Ciencia, Tecnología y Futuro* **1998**, *1*, 65–73.

26. Yang, H.; Ring, Z.; Briker, Y.; McLean, N.; Friesen, W.; Fairbridge, C. Neural network prediction of cetane number and density of diesel fuel form its chemical composition determined by LC and GC-MS. *Fuel* **2002**, *81*, 65–74. [CrossRef]

27. Masy, T.; Caterina, D.; Tromme, O.; Lavigne, B.; Thonart, P.; Hiligsmann, S.; Nguyen, F. Electrical resistivity tomography to monitor enhanced biodegradation of hydrocarbons with *Rhodococcus erythropolis* T902.1 at a pilot scale. *J. Contam. Hydrol.* **2016**, *184*, 1–13. [CrossRef] [PubMed]

28. Sutton, N.B.; van Gaans, P.; Langenhoff, A.A.M.; Maphosa, F.; Smidt, H.; Grotenhuis, T.; Rijnaarts, H.H.M. Biodegradation of aged diesel soil matrixes: Impact of environmental conditions and bioavailability on microbial remediation capacity. *Biodegradation* **2013**, *24*, 487–498. [CrossRef] [PubMed]

29. Cui, J.-Q.; He, Q.-S.; Liu, M.-H.; Chen, H.; Sun, M.-B.; Wen, J.-P. Comparative Study on Different Remediation Strategies Applied in Petroleum-Contaminated Soils. *Int. J. Environ. Res. Public Health* **2020**, *17*, 1606. [CrossRef] [PubMed]

30. Decreto Legislativo, n.; 152 del 3 Aprile 2006 "Norme in Materia Ambientale", Supplemento Ordinario alla "Gazzetta Ufficiale" n. 88 del 14 Aprile 2006. Available online: https://www.gazzettaufficiale.it/dettaglio/codici/materiaAmbientale (accessed on 5 December 2020).